

Supporting Information for  
**Restricted rupture evolution of the 2022  $M_w$  6.7 Luding China earthquake**

Yaping Hu<sup>1</sup>, Yuji Yagi<sup>2,3</sup>, Ryo Okuwaki<sup>2,3</sup>, Ryo Yamaguchi<sup>4</sup>, Hangyu Gao<sup>5</sup>

<sup>1</sup>School of Geophysics and Measurement-control Technology, East China University of Technology, NO.418, Guanglan Street, Nanchang, Jiangxi, China

<sup>2</sup>Faculty of Life and Environmental Sciences, University of Tsukuba, Tennodai 1-1-1, Tsukuba, Ibaraki 305–8572, Japan

<sup>3</sup>Mountain Science Center, University of Tsukuba, Tennodai 1-1-1, Tsukuba, Ibaraki 305–8572, Japan

<sup>4</sup>College of Geoscience, School of Life and Environmental Sciences, University of Tsukuba, Tennodai 1-1-1, Tsukuba, Ibaraki 305–8572, Japan

<sup>5</sup>Graduate School of Science and Technology, University of Tsukuba, Tennodai 1-1-1, Tsukuba, Ibaraki 305–8572, Japan

Contents

Table S1: Velocity model used for calculating Green's function

Table S2: Alternative velocity model used for calculating Green's function

Figure S1: Full snapshots of potency-rate density tensor distribution

Figure S2: Waveform fits

Figure S3: Alternative solution based on CRUST1.0 velocity model

Figure S4: Full snapshots of potency-rate density tensor distribution from the modelling with a parallel fault

Figure S5: Summary for the model with a parallel fault

**Table S1.** Velocity model of Xu et al. (2013) used for calculating Green's function

$V_P$ (km/s)	$V_S$ (km/s)	Density ( $10^3 \text{ kg/m}^3$ )	Thickness (km)
4.600	2.656	2.615	3.0
6.050	3.493	2.760	9.0
6.170	3.562	2.679	10.0
6.250	3.608	2.835	8.0
6.550	3.782	2.835	10.0
6.800	3.926	2.977	18.0
7.800	4.503	3.175	0*

\*0-km thickness means the semi-infinite velocity layer below the moho depth

**Table S2.** Velocity model of CRUST 1.0 (Laske et al., 2013) without soft layers used for calculating Green's function

$V_P$ (km/s)	$V_S$ (km/s)	Density ( $10^3 \text{ kg/m}^3$ )	Thickness (km)
6.10	3.55	2.74	20.66
6.30	3.65	2.78	20.13
7.00	3.99	2.95	8.78
8.04	4.47	3.31	0*

\*0-km thickness means the semi-infinite velocity layer below the moho depth

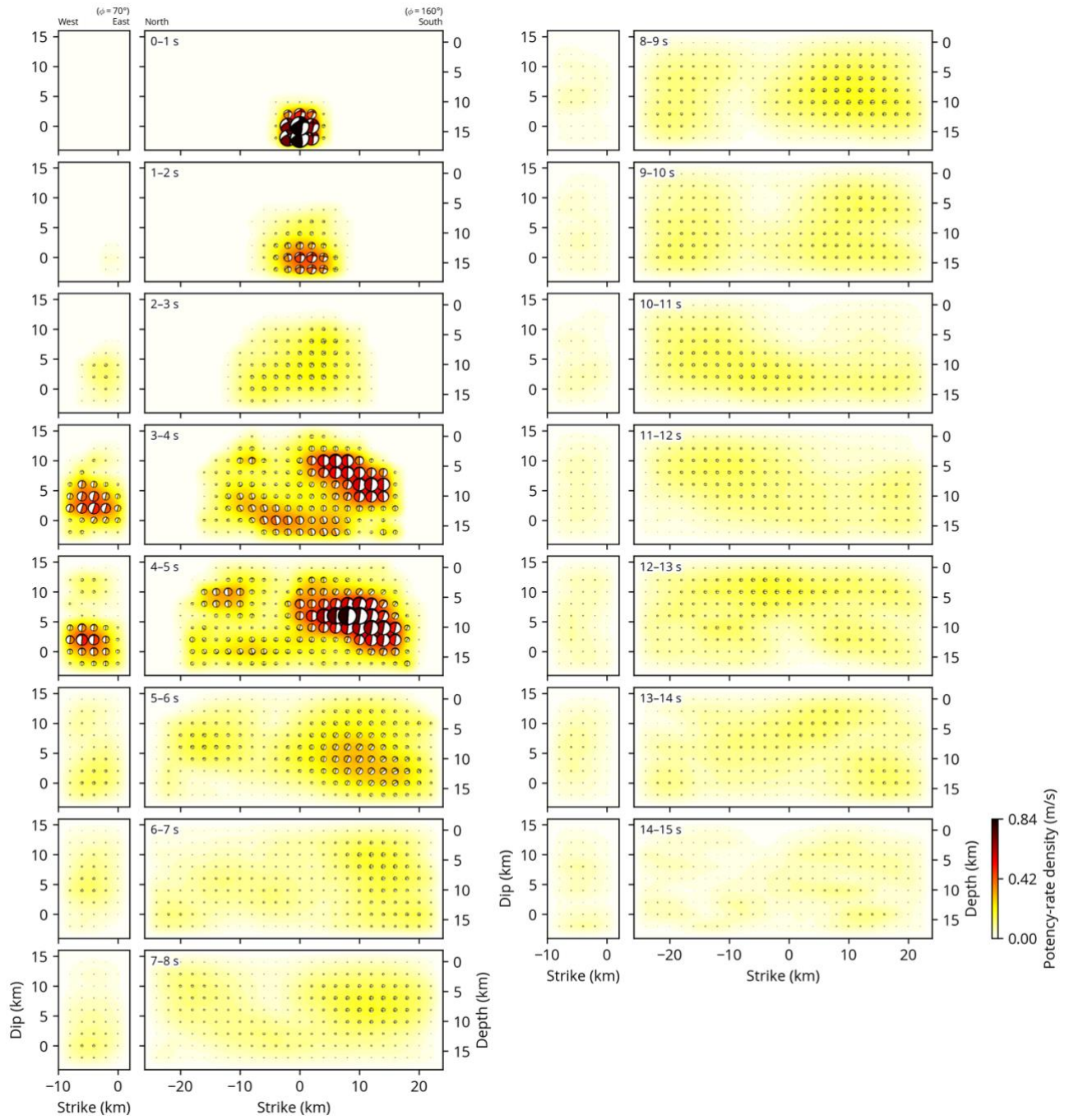


Figure S1. Full snapshots of potency-rate density tensor distribution. The strike of the model fault ( $\phi$ ) is denoted in on each panel. The beachballs in the left and right figures are shown in cross-sectional views from the west-southwest side and south-southeast side, respectively.

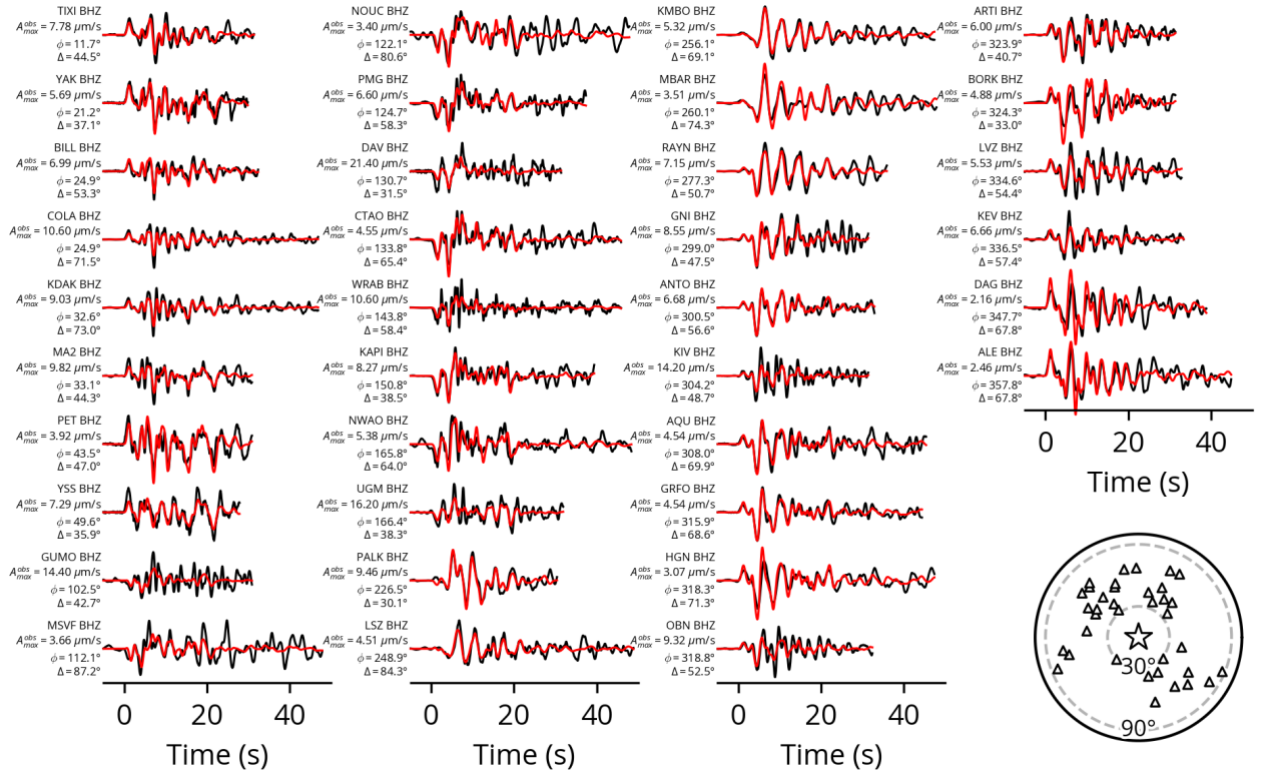


Figure S2. Waveform fitting for the estimated source model shown in Figs. 2–4. Observed waveform (black trace) and synthetic waveform reconstructed using the estimated source model (red trace) at each station. Each waveform panel is labelled with the station name, component, maximum amplitude, azimuth ( $\phi$ ), and epicentral distance ( $\Delta$ ). The bottom right panel shows the station distribution (triangles). Dashed circles show epicentral distance of 30° and 90°. The star indicates the epicentre of the 2022 Luding earthquake.

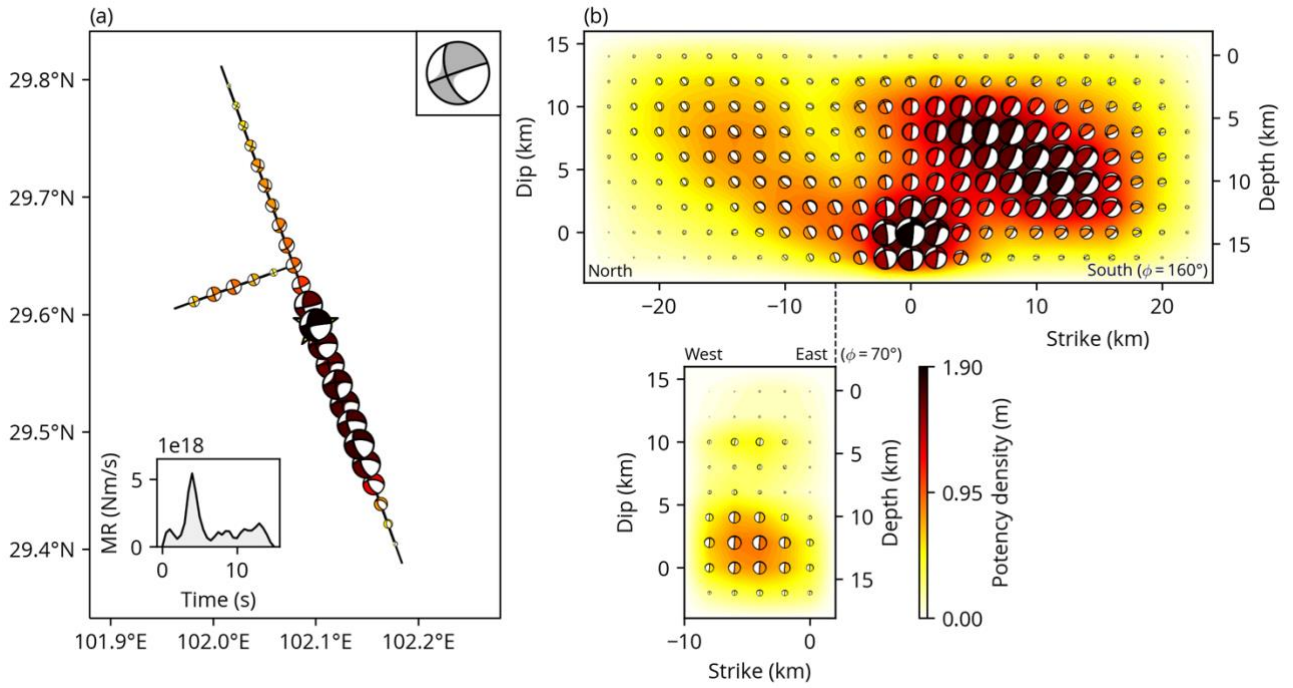


Figure S3. Summary of the reproducibility test using an alternative structural model based on CRUST1.0 velocity model (Table S2) (Laske et al., 2013). (a) Potency density tensor distribution in a map view. The yellow star denotes the epicentre. The beach ball in the upper right corner indicates the total moment tensor of our solution. The inset shows the moment-rate function. The beachballs show the lower-hemisphere projection of the potency density tensor. Only shown are the maximum potency-density tensors along depth (see all the potency density tensors in a cross-sectional view in Fig. S3b). (b) The cross section of the potency density tensor distribution. The strike of the model fault ( $\phi$ ) is denoted in upper right of each panel. The beachballs in the upper and bottom panels are shown in cross-sectional views from the west-southwest side and south-southeast side, respectively.



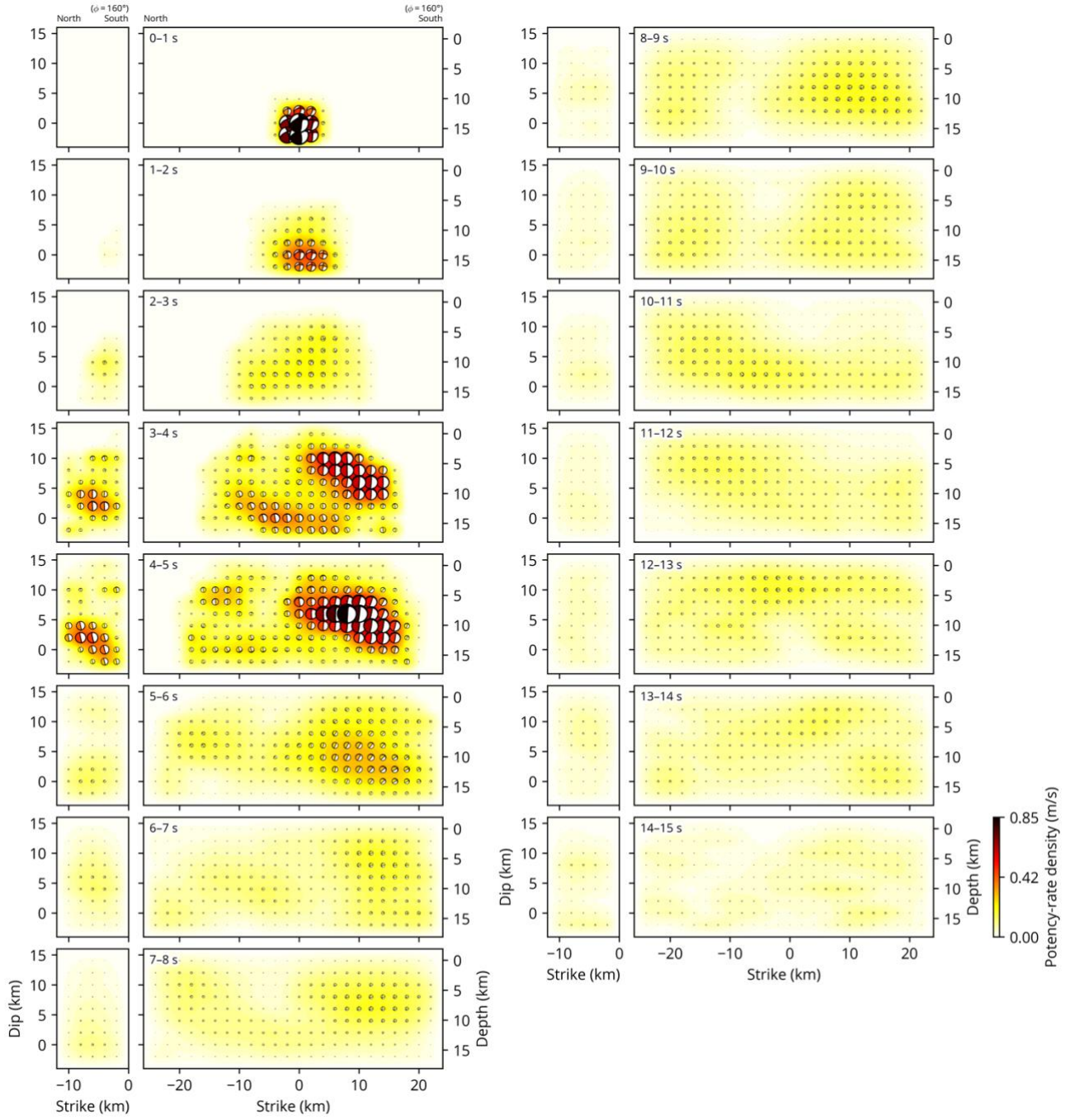


Figure S4. Full snapshots of potency-rate density tensor distribution for the model with the parallel additional model fault. The strike of the model fault ( $\phi$ ) is denoted on each panel. The beachballs are shown in a cross-sectional view from the west-southwest side.

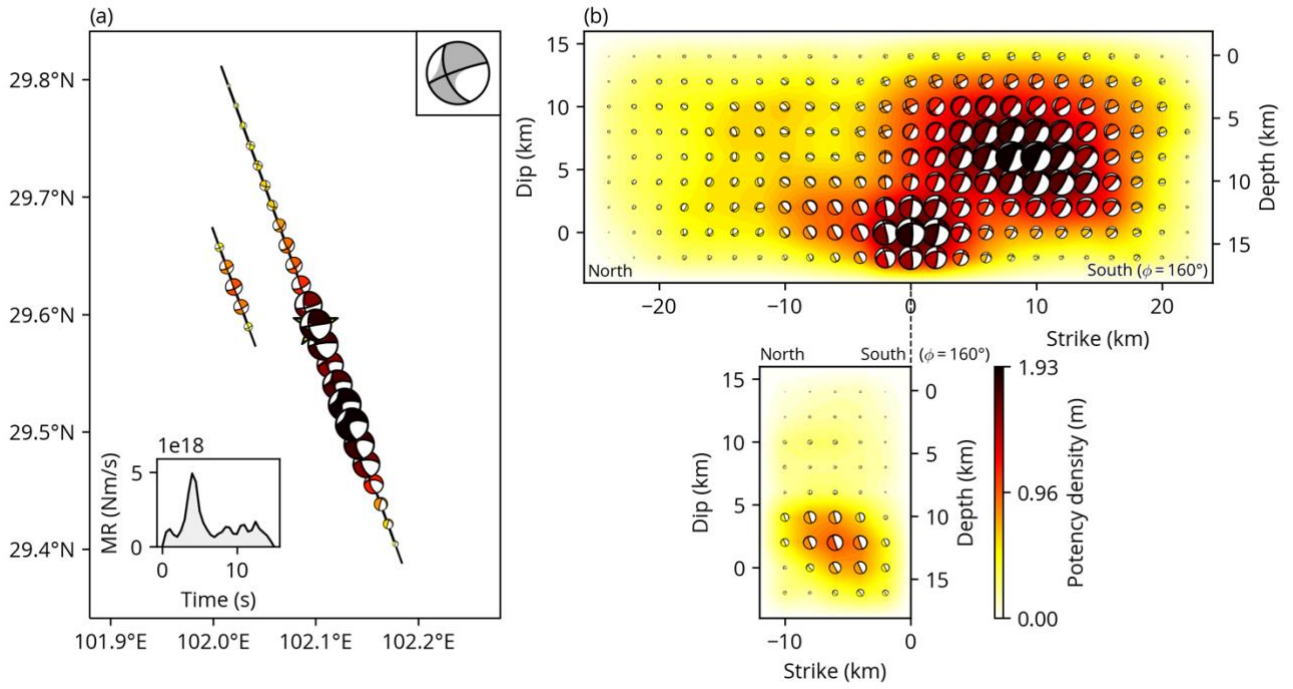


Figure S5. Summary of the inversion result when strike of the additional model plane is set parallel to the main model plane. (a) Potency density tensors distribution in a map projection. The yellow star denotes the epicentre. The beach ball in the upper right corner indicates the total moment tensor of our solution. The inset shows the moment-rate function. The beachballs show the lower-hemisphere projection of the potency density tensor. Only shown are the maximum potency-density tensors along depth. (b) The cross section of the potency density tensor distribution. The strike of the model fault ( $\phi$ ) is denoted in upper right of each panel. The beachballs are shown in cross-sectional view from the and west-southwest side.

## References

- Xu, J., Shao, Z. G., Ma, H. S., & Zhang, L. P. (2013). Evolution of Coulomb stress and stress interaction among strong earthquakes along the Xianshuihe fault zone (in Chinese). *Chinese Journal of Geophysics*, 56(4), 1146-1158. <https://doi.org/10.6038/cjg20130410>
- Laske, G., Masters, T. G., Ma, Z., & Pasyanos, M. (2013). Update on CRUST1.0 - A 1-degree Global Model of Earth's Crust. *Geophys. Res. Abstr.* 15, *Abstr. EGU2013-2658*, 15, Abstract EGU2013-2658. Retrieved from <http://igppweb.ucsd.edu/~gabi/rem.html>